Observation of self-trapping and rotation of higher-band gap solitons in two-dimensional photonic lattices

Shiqiang Xia,[1] Daohong Song,[1] Yuanyuan Zong,[1] Liqin Tang,[1,*] and Zhigang Chen[1,2]

[1]*The MOE Key Laboratory of Weak-Light Nonlinear Photonics, TEDA Applied Physics Institute and School of Physics, Nankai University, Tianjin 300457, China*

[2]*Department of Physics and Astronomy, San Francisco State University, San Francisco, California 94132, USA*

* *tanya@nankai.edu.cn*

Abstract: We demonstrate self-trapping and rotation of higher-band dipole and quadruple-like gap solitons by single-site excitation in a two-dimensional square photonic lattice under self-focusing nonlinearity. Experimental results show that the second-band dipole gap solitons reside in the first photonic (Bragg reflection) gap, whereas the quadruple-like gap solitons are formed in an even higher photonic gap, resulting from modes of the third-band. Moreover, both dipole and quadruple-like gap solitons exhibit dynamical rotation around the lattice principle axes and the direction of rotation is changing periodically during propagation, provided that they are excited under appropriate initial conditions. In the latter case, the nonlinear rotation is accompanied by periodic transitions between quadruple and doubly-charged vortex states. Our numerical simulations find good agreement with the experimental observations.

©2015 Optical Society of America

OCIS codes: (190.6135) Spatial solitons; (190.4420) Nonlinear optics, transverse effects in.

References and links

1. D. N. Christodoulides, F. Lederer, and Y. Silberberg, "Discretizing light behaviour in linear and nonlinear waveguide lattices," Nature **424**(6950), 817–823 (2003).
2. F. Lederer, G. I. Stegeman, D. N. Christodoulides, G. Assanto, M. Segev, and Y. Silberberg, "Discrete solitons in optics," Phys. Rep. **463**(1-3), 1–126 (2008).
3. Z. Chen, M. Segev, and D. N. Christodoulides, "Optical spatial solitons: historical overview and recent advances," Rep. Prog. Phys. **75**(8), 086401 (2012).
4. I. L. Garanovich, S. Longhi, A. A. Sukhorukov, and Y. S. Kivshar, "Light propagation and localization in modulated photonic lattices and waveguides," Phys. Rep. **518**(1-2), 1–79 (2012).
5. H. S. Eisenberg, Y. Silberberg, R. Morandotti, A. R. Boyd, and J. S. Aitchison, "Discrete spatial optical solitons in waveguide arrays," Phys. Rev. Lett. **81**(16), 3383–3386 (1998).
6. N. K. Efremidis, S. Sears, D. N. Christodoulides, J. W. Fleischer, and M. Segev, "Discrete solitons in photorefractive optically induced photonic lattices," Phys. Rev. E Stat. Nonlin. Soft Matter Phys. **66**(4), 046602 (2002).
7. J. W. Fleischer, M. Segev, N. K. Efremidis, and D. N. Christodoulides, "Observation of two-dimensional discrete solitons in optically induced nonlinear photonic lattices," Nature **422**(6928), 147–150 (2003).
8. D. Neshev, E. Ostrovskaya, Y. Kivshar, and W. Krolikowski, "Spatial solitons in optically induced gratings," Opt. Lett. **28**(9), 710–712 (2003).
9. H. Martin, E. D. Eugenieva, Z. Chen, and D. N. Christodoulides, "Discrete solitons and soliton-induced dislocations in partially coherent photonic lattices," Phys. Rev. Lett. **92**(12), 123902 (2004).
10. D. Mandelik, R. Morandotti, J. S. Aitchison, and Y. Silberberg, "Gap solitons in waveguide arrays," Phys. Rev. Lett. **92**(9), 093904 (2004).
11. D. Neshev, A. A. Sukhorukov, B. Hanna, W. Krolikowski, and Y. S. Kivshar, "Controlled generation and steering of spatial gap solitons," Phys. Rev. Lett. **93**(8), 083905 (2004).
12. G. Bartal, O. Manela, O. Cohen, J. W. Fleischer, and M. Segev, "Observation of second-band vortex solitons in 2D photonic lattices," Phys. Rev. Lett. **95**(5), 053904 (2005).
13. F. Chen, M. Stepić, C. E. Rüter, D. Runde, D. Kip, V. Shandarov, O. Manela, and M. Segev, "Discrete diffraction and spatial gap solitons in photovoltaic $LiNbO_3$ waveguide arrays," Opt. Express **13**(11), 4314–4324 (2005).
14. C. Lou, X. Wang, J. Xu, Z. Chen, and J. Yang, "Nonlinear spectrum reshaping and gap-soliton-train trapping in

#232806 - $15.00 USD Received 21 Jan 2015; revised 7 Feb 2015; accepted 9 Feb 2015; published 11 Feb 2015
© 2015 OSA

optically induced photonic structures," Phys. Rev. Lett. **98**(21), 213903 (2007).
15. D. Kip, C. E. Rüter, R. Dong, Z. Wang, and J. Xu, "Higher-band gap soliton formation in defocusing photonic lattices," Opt. Lett. **33**(18), 2056–2058 (2008).
16. R. Dong, C. E. Rüter, D. Song, J. Xu, and D. Kip, "Formation of higher-band dark gap solitons in one dimensional waveguide arrays," Opt. Express **18**(26), 27493–27498 (2010).
17. Z. Shi and J. Yang, "Solitary waves bifurcated from Bloch-band edges in two-dimensional periodic media," Phys. Rev. E Stat. Nonlin. Soft Matter Phys. **75**(5 Pt 2), 056602 (2007).
18. X. Wang, L. Daniel, Z. Chen, J. Wang, and J. Yang, "Nonlinear dipole rotation/oscillation in anisotropic lattices," in Frontiers in Optics 2008/Laser Science XXIV/Plasmonics and Metamaterials/Optical Fabrication and Testing, OSA Technical Digest (CD) (Optical Society of America, 2008), paper FThD5.
19. S. Xia, D. Song, L. Tang, C. Lou, and Y. Li, "Self-trapping and oscillation of quadruple beams in high band gap of 2D photonic lattices," Chin. Opt. Lett. **11**(9), 090801 (2013).
20. J. Yang, I. Makasyuk, A. Bezryadina, and Z. Chen, "Dipole and quadruple solitons in optically induced two-dimensional photonic lattices: theory and experiment," Stud. Appl. Math. **113**(4), 389–412 (2004).
21. Z. Chen, A. Bezryadina, I. Makasyuk, and J. Yang, "Observation of two-dimensional lattice vector solitons," Opt. Lett. **29**(14), 1656–1658 (2004).
22. D. Träger, R. Fischer, D. N. Neshev, A. A. Sukhorukov, C. Denz, W. Królikowski, and Y. S. Kivshar, "Nonlinear Bloch modes in two-dimensional photonic lattices," Opt. Express **14**(5), 1913–1923 (2006).
23. A. Bezryadina, E. Eugenieva, and Z. Chen, "Self-trapping and flipping of double-charged vortices in optically induced photonic lattices," Opt. Lett. **31**(16), 2456–2458 (2006).
24. E. Eugenieva, D. Song, A. Bezryadina, P. Zhang, Z. Chen, and N. B. Abraham, "Self-trapping and stabilization of doubly-charged optical vortices in two-dimensional photonic lattices," J. Mod. Opt. **57**(14–15), 1377–1387 (2010).

1. Introduction

Optical spatial lattice solitons, localized structures resulting from the exact balance between periodicity and nonlinearity in photonic lattices, have attracted a great deal of interest in the past dozen years [1–4]. Different types of lattice solitons including discrete solitons, band gap solitons and even higher-band gap solitons have been extensively studied both theoretically and experimentally [5–14]. More specifically, in some cases discrete lattice solitons can be formed in the semi-infinite gap near the top of the first Bloch band under a self-focusing nonlinearity. In some other cases, fundamental gap solitons residing in the first Bragg reflection (photonic) gap can be excited either from modes of the first band through balance between anomalous diffraction and defocusing nonlinearity or from modes of the second band through balance between normal diffraction and focusing nonlinearity. Thus far, lattice solitons located in higher photonic band gap are only experimentally observed in one-dimensional (1D) defocusing photonic lattices [15,16]. In two-dimensional (2D) lattices, on the other hand, higher-gap solitons have been theoretically proposed [17] but not experimentally realized to our knowledge, most probably due to the difficulties in opening the higher-band gaps and exciting the pure modes from the higher-bands in 2D photonic lattices. Moreover, many interesting features such as rotation of dipole gap solitons [18] are expected to occur only in higher dimensions. Recently, we have also predicated the formation and rotation of higher-band quadruple-like solitons residing in the second Bragg reflection gap of the 2D square lattices [19], but experimental demonstration of such higher-band gap solitons remains to be a challenge.

In this paper, we present the experimental demonstration of self-trapping and rotation of second-band dipole and third-band quadruple-like lattice solitons in 2D photonic lattices induced with a self-focusing nonlinearity. The input dipole or quadruple beam with desired phase structure is launched at single lattice site. In the absence of nonlinearity, the dipole (quadruple) beam exhibits linear discrete diffraction which characterizes the feature of the corresponding second (third) band Bloch modes. Under appropriate conditions of nonlinearity, the probe beam self-traps into a gap soliton with its spatial spectrum concentrated on the corresponding high-symmetry points in the Brillouin Zone (BZ). Specifically, the dipole gap soliton forms in the first Bragg reflection gap, while the quadruple-like soliton forms in the second Bragg reflection gap. Furthermore, different from previously observed dipole soliton rotation in anisotropic lattices [18], here we demonstrate the rotation of dipole gap solitons in a 2D square lattice without intentionally introducing the anisotropy to the lattice. Importantly, the

#232806 - $15.00 USD Received 21 Jan 2015; revised 7 Feb 2015; accepted 9 Feb 2015; published 11 Feb 2015
© 2015 OSA

rotation of localized quadruple states can be experimentally observed only by changing the initial orientation of the incident beams relative to the symmetry axes of the lattice. Our experimental observations are corroborated by numerical results, representing another example of continued success of investigating spatial beam dynamics with the platform of optically induced photonic lattices.

2. Experimental methods

Our experimental setup is shown in Fig. 1, which is similar to those used earlier for observation of discrete dipole or vector solitons [20,21], except that we now use a spatial light modulator (SLM) to generate the probe beam. A laser beam (532nm) is divided into three parts (shown with three red arrows): the lattice-forming beam, the probe beam and the reference beam. In the first path (going through the amplitude mask), a partially spatially incoherent beam is generated by using a rotating diffuser. A biased photorefractive crystal (SBN: 5mm × 10mm × 5mm) is employed to provide a self-focusing nonlinearity. To generate a 2D square lattice, we use an amplitude mask to spatially modulate the otherwise uniform beam after the diffuser. The lattice beam is ordinarily polarized, which remains invariant during propagation through the crystal. The second path is the probe beam, which is extraordinarily polarized and sent into the SLM imprinted with desired phase information for generation of dipole and quadruple beams. Taking advantage of the photorefractive non-instantaneous response, we monitor the linear and nonlinear transport of the probe beam simply by recording its instantaneous (before nonlinear self-action) and steady-state (after self-action) output patterns. The input and output images are taken by a CCD camera (CCD-1) and their phase profiles are monitored by interfering them with a tilted broad plane wave (the third path of the laser beam). In addition, the Fourier spectrum of the output beams can be visualized by another CCD camera (CCD-2) when needed.

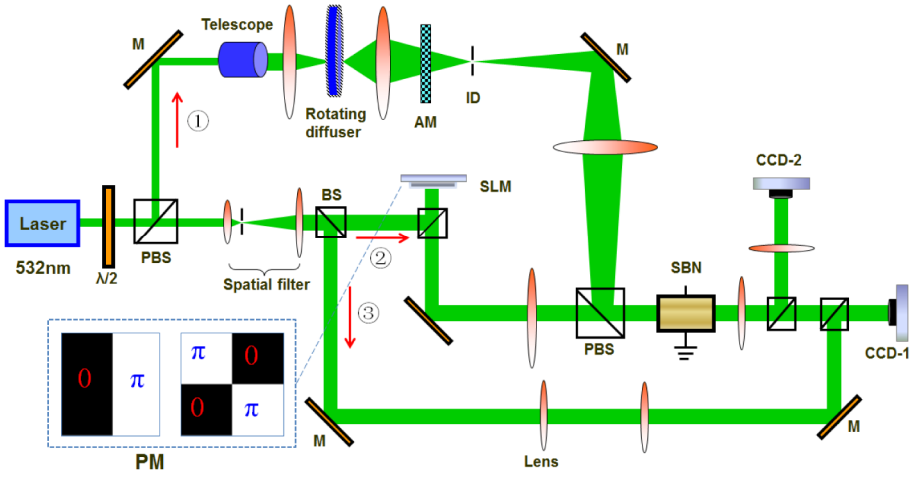

Fig. 1. Experimental setup: (P)BS, (polarizing) beam splitter; ID, iris diaphragm; M, mirror; SBN, strontium barium niobate crystal; SLM, phase-only spatial light modulator; AM, amplitude mask; PM, phase masks displayed in SLM to generate out-of phase dipole (left) and quadruple (right) beams. Red arrows 1, 2, 3 indicate the paths of the lattice-inducing beam, the probe beam and the reference beam, respectively.

As mentioned, the incident dipole and quadruple beams have nonuniform phase structures, i.e., for the dipole beam, the two humps are out-of phase, and for the quadruple beam, the diagonal humps are in-phase, but the adjacent humps have a π-phase difference. The experimental realization of such probe beams are achieved by using a phase-only SLM encoded with numerically calculated phase mask as shown in Fig. 1. After modulation by the phase mask, a broad Gaussian beam is transformed into a dipole beam with two peaks or a quadruple beam with four peaks. Note that different from prior experiments on discrete solitons [20,21], in

#232806 - $15.00 USD Received 21 Jan 2015; revised 7 Feb 2015; accepted 9 Feb 2015; published 11 Feb 2015
© 2015 OSA

all our current experiments, the probe beam is focused to excite only one lattice site. Consequently, the spectrum of the probe beam extends to cover higher-bands so that higher-band Bloch modes can be excited. Furthermore, simply by rotating the phase masks on the SLM, orientations of the incident dipole/quadruple beams relative to the lattice axes can be changed at will, permitting the investigation of soliton propagation under different initial conditions.

3. Experimental and numerical results

3.1 Self-trapping and rotation of dipole gap solitons

In this section, we study self-trapping and rotation of second-band dipole solitons residing in the first Bragg reflection gap in optically induced 2D square photonic lattices. In these experiments, the square lattice (of spacing about 28μm) beam is diagonally oriented, and the intensity of the dipole beam is about four times weaker than that of the lattice beam.

First, we present self-trapping of dipole gap soliton orientated in horizontal direction (horizontal excitation). Typical experimental results are shown in the top panels of Fig. 2. An out-of phase dipole beam is launched into the same lattice site [Fig. 2(a1)], and in this case, it excites the second band Bloch modes [17,22]. At a low bias field of 120V/mm, the dipole beam undergoes linear discrete diffraction [Fig. 2(a2)]. Along the direction of the principal axes of the square lattice, dipole "tails" beyond the central two spots can be seen, with an intensity pattern characteristic to the Bloch modes at the *X*-points of the second band [17,22]. At a high bias field of 180V/mm, the dipole beam is trapped at the output of the 10-mm long crystal, leading to the formation of dipole gap soliton [Fig. 2(a3)]. Phase measurement (inset in [Fig. 2(a3)]) by interfering the output with an inclined plane wave indicates that the initial out-phase structure is well preserved when the dipole soliton is formed. Moreover, spatial spectrum of the self-trapped dipole soliton is also measured. It is shown that most of the spectrum power is located alongside the first BZ and close to four *X*-points [Fig. 2(a4)], confirming again the dipole gap soliton is bifurcated from the second Bloch band. For comparison, we numerically study the formation of dipole gap soliton with the parameters similar to those from the experiment. The numerical model is a nonlinear wave equation with a 2D square lattice potential under self-focusing photorefractive nonlinearity and can be described by the following equation [19–22]:

$$i\partial_z\psi(x,y,z)+\frac{1}{2k}\nabla^2\psi(x,y,z)+\frac{k}{n_e}\Delta n_e\psi(x,y,z)=0. \qquad (1)$$

Here ψ is the envelope of the optical field; (x,y) are transverse coordinates and z is the longitudinal propagation distance into the photonic lattice; k is the wavenumber within the medium; n_e is the extraordinary refractive index of bulk photorefractive SBN crystal and $\Delta n_e=-\frac{1}{2}n_e^3\gamma_{33}\frac{E_0}{1+I_l+|\psi|^2}$ is the nonlinear refractive index change; γ_{33} is the electro-optic coefficient; E_0 is the applied direct current (dc) field, and I_l is the lattice intensity; ∇^2 is the Laplacian in the transverse (x,y) plane. Numerical results are shown in the bottom panels of Fig. 2 after the same propagation length (10mm) for direct comparison. One can see that there is an excellent agreement between experimental and numerical results.

#232806 - $15.00 USD Received 21 Jan 2015; revised 7 Feb 2015; accepted 9 Feb 2015; published 11 Feb 2015
© 2015 OSA

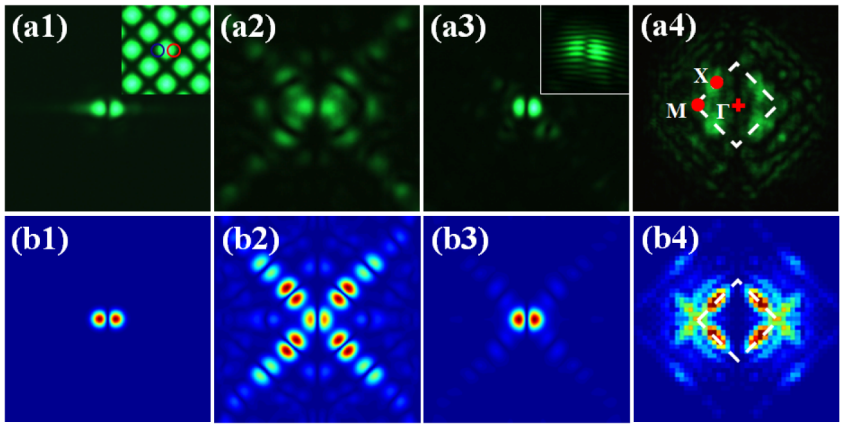

Fig. 2. Experimental (top) and numerical (bottom) results of self-trapping of dipole gap solitons. (a1), (b1) input dipole beams; (a2), (b2) linear diffractions; (a3), (b3) nonlinear outputs; and (a4), (b4) *k*-space spectra of (a3), (b3). Inset in (a1) shows lattice pattern with circles marking the dipole input position. Inset in (a3) shows interferogram of the corresponding nonlinear output. White dashed squares in (a4), (b4) represent the first Brillouin Zone of the square lattice.

A fascinating property of dipole gap solitons is that they can rotate around particular axes of the lattices when the orientation of the incident dipole beam is slightly twisted relative to the symmetry axes of the lattices. To demonstrate the dipole gap soliton rotation experimentally, we launch an input dipole beam with an initial ± 10° angle relative to the horizontal axis in Fig. 2(a1) and keep other experimental parameters unchanged. Results are presented in Fig. 3, where Figs. 3(a) and 3(c) show the input dipole beams and Figs. 3(b) and 3(d) show the corresponding nonlinear output. It can be clearly seen that, with the same nonlinear excitation, the input dipole beam self-traps into a dipole gap soliton, but it rotates oppositely (clockwise in [Fig. 3(b)] and counterclockwise in [Fig. 3(d)]) depending on its initial orientation.

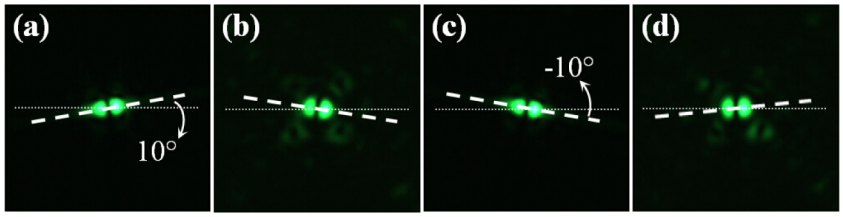

Fig. 3. Experimental results of dipole gap soliton rotation. (a), (c) input dipole beams with different orientations; (b), (d) nonlinear output of dipole gap solitons. The long thin dashed lines mark the horizontal direction, while the short thick lines illustrate the dipole orientation.

Experimentally, it is a challenge to explore the rotation dynamics in detail due to a limited propagation distance (crystal length). Our numerical analysis suggests that the dipole rotation will not stay along one direction, but it will rotate back and forth so long as it propagates for sufficient long distances. As an example, we consider the situation in Fig. 3(a) for demonstration and set the propagation distance to Z = 140mm. Results are illustrated in Fig. 4 (see Media 1). Figure 4(a) shows the input dipole beam and Figs. 4(b) and 4(c) represent nonlinear localized states where the rotation starts to reverse. It is shown that the dipole soliton rotates clockwise at first until it transforms into the state depicted in Fig. 4(b) (Z = 55mm). Then, the rotating direction is reversed and the dipole soliton starts to rotate counterclockwise, transforming into the state at Z = 110mm [Fig. 4(c)]. Thereafter, the dipole soliton will repeat such rotation periodically during propagation. In fact, similar phenomena have also been observed in our experiment for the dipole solitons orientated in vertical direction. Our analysis

#232806 - $15.00 USD Received 21 Jan 2015; revised 7 Feb 2015; accepted 9 Feb 2015; published 11 Feb 2015
© 2015 OSA

shows that the dipole solitons orientated in lattice principle axes and diagonal axes (i.e., horizontal and vertical axes) are stable, while in other initial orientations the dipole solitons tend to rotate around the closest horizontal and vertical axes (Note that the principle axes of the square lattice are oriented in the 45° diagonal directions as shown in the insert of the Fig. 2). One possible explanation for such dipole rotation is that the dipole solitons with an initial angle relative to one of the lattice axes can be considered as a coherent superposition of two stationary dipole solitons along two perpendicular directions (one is the stable component oriented in horizontal direction, and the other in vertical direction, and the two dipoles have the same propagation constant) with a different ratio between the two components. Different angles of the dipole indicate different ratios of the two components. Periodic energy exchange between the two components via nonlinearity leads to the dynamic rotation or oscillation.

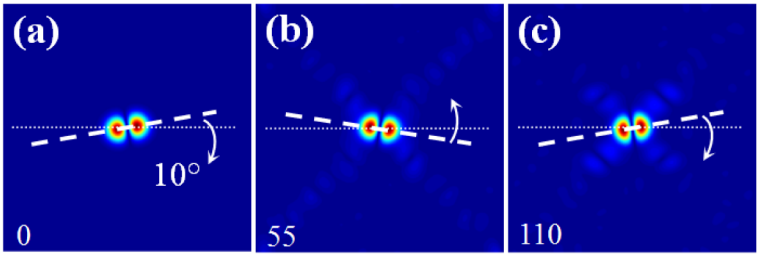

Fig. 4. Simulation results of dipole soliton rotation (Media 1). (a) input dipole beam with a 10° initial angle relative to the horizontal direction; (b), (c) nonlinear output patterns of localized dipole states taken when the direction of rotation starts to reverse.

3.2 Self-trapping and rotation of higher-band quadruple-like solitons

Similar experiments are conducted for the study of higher-band quadruple-like solitons by reconfiguring the initial phase of the input probe beam. It is important to note that, in order to open the high Bragg reflection gap and excite the higher-band Bloch modes of square lattice, a relatively higher intensity of the lattice beam (about 1.3 times) and a larger lattice spacing (about 34μm) are employed comparing with the above dipole soliton experiments. Typical experimental results of higher-band quadruple-like gap soliton are shown in the top row of Fig. 5. An out-of phase quadruple beam is launched into the lattice and focused to excite a single-site as shown in Fig. 5(a). At a low bias field of 140V/mm, the quadruple beam exhibits linear discrete diffraction [Fig. 5(b)] with most of the energy coupled to nearby waveguides at the output of the crystal. At a high bias field of 220V/mm, the quadruple beam is self-trapped into a quadruple-like gap soliton with "quadruple" tails along the two principle axes [Fig. 5(c)], characterizing the Bloch modes of the third Bloch band [17,19]. Note that in the nonlinear case, both the intensity pattern [Fig. 5(c)] and the interferogram [Fig. 5(d)] clearly show that the phase structure at the output is well preserved. More importantly, the nonlinear power spectrum [Fig. 5(e)] reshapes and the energy transfers to the boundary of the second BZ, suggesting that the observed quadruple-like soliton resides in the second Bragg reflection gap. In fact, quite different from all previously observed solitons in 2D lattices, such a higher-gap quadruple-like soliton is bifurcated from the *X* points of the third Bloch band [17,19], which has not been experimentally demonstrated before. These observations are compared with our numerical simulation shown in the bottom row of Fig. 5 using the parameters similar to those of the experiments. It can be clearly seen that the numerical results are again in good agreement with our experimental results. Simulation also shows that the spectrum tends to settle into regions close to the four points of the second BZ boundary.

#232806 - $15.00 USD Received 21 Jan 2015; revised 7 Feb 2015; accepted 9 Feb 2015; published 11 Feb 2015
© 2015 OSA

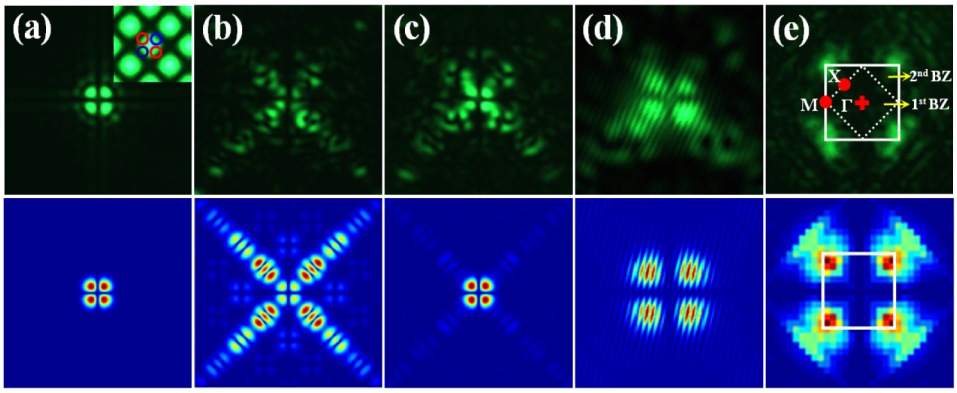

Fig. 5. Experimental (top row) and numerical (bottom row) results showing the formation of third-band quadruple-like gap soliton. Shown are (a) input quadruple beam; (b) linear diffraction; (c) nonlinear output; and (d), (e) corresponding interferogram and nonlinear Fourier spectrum. The dashed and solid white squares in (e) mark the 1st and 2nd BZ, respectively. (d) is zoomed-in with respected to (c) for better visualization. Inset in (a) shows the lattice pattern with circles marking the quadruple input position.

Next, the quadruple orientation is changed while keeping other experimental parameters fixed for investigation of the quadruple-like soliton rotation. Results are presented in Fig. 6. Compared with the excitation shown in Fig. 5(a), the input quadruple beam in Figs. 6(a) and 6(c) has an initial ± 5° angle relative to the lattices principle axes (Note that different from the dipole soliton rotation experiment, here we choose the lattices principle axes as the reference axes for better illustrating the rotating angle). It can be seen that the quadruple beams still can be self-trapped with the same nonlinearity but the orientations cannot be preserved [Figs. 6(b) and 6(d)] at the output of the crystal. So, similar to dipole gap soliton rotation, we find that such higher-band quadruple-like solitons also experience self-rotation once their orientation is deviated from the stable configuration.

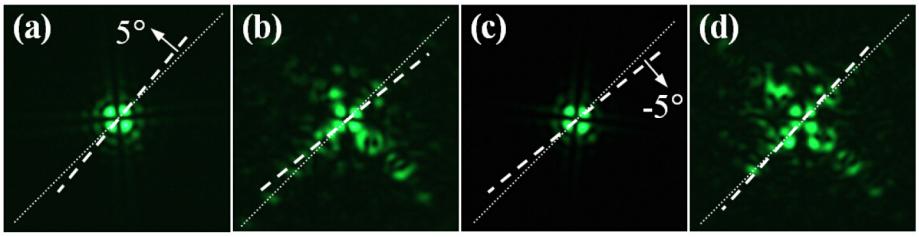

Fig. 6. Experimental results showing rotation of nonlinear localized quadruple-like gap solitons. (a), (c) the input quadruple beams with an ± 5° initial angles relative to the lattice principle axes; and (b), (d) their corresponding nonlinear outputs. The long thin dashed lines mark the direction of lattices principle axes, while the short thick lines illustrate the quadruple orientation.

To explore the dynamics of the quadruple-like soliton rotation in detail, we also simulated the propagation of the quadruple-like soliton over a longer distance. We take the situation in Fig. 6(a) as an example. Our numerical analysis not only suggests that the quadruple-like soliton will experience rotation similar to dipole solitons but also reveals that the localized quadruple state becomes a rotating doubly-charged vortex (DCV) during rotation and undergoes charge-flipping when the rotating direction is reversed [23,24]. Typical results are shown in Fig. 7(see Media 2). Figure 7(a) depicts the input quadruple beam with the lattice pattern shown in the background and Fig. 7(b) represents the side-view of propagation to z = 180mm. By analyzing the output states at different locations, we can find that the localized mode rotates around the principle lattices axis. Figures 7(c)-7(f) depict the output intensities

#232806 - $15.00 USD Received 21 Jan 2015; revised 7 Feb 2015; accepted 9 Feb 2015; published 11 Feb 2015
© 2015 OSA

and phase structures corresponding to the propagation length Z = 96mm, 121mm, 145mm, 169mm, where the four white dashed lines in Fig. 7(b) are located. Figures 7(c) and 7(e) are quadruple states where the rotation starts to reverse. The localized output state at z = 96mm is similar to the input and it rotates counterclockwise. Nevertheless, the intensity and phase structure at z = 121mm illustrate that the quadruple localized state develops into a vortex with a 4π helical phase structure around the singular point (i.e., m = 2 vortex). Then, the DCV continues to rotate counterclockwise and breaks into a quadruple localized structure again until it propagates to z = 145mm [Fig. 7(e)]. Thereafter, such a quadruple state rotates clockwise, followed by the reappearance of a DCV with opposite charges m = –2, i.e., a charge-flipping occurs. In short, the entire intensity and phase distribution of the localized state varies during propagation, as represented by the periodic appearance of a quadruple structure, a m = + 2 vortex, a quadruple structure again, and then a m = –2 vortex. To verify the phase structure, interferograms of the output states are shown in the bottom row of Fig. 7, which clearly shows that the out-of phase feature in the quadruple localized states [Figs. 7(c) and 7(e)] as well as charge-flipping during propagation [Figs. 7(d) and 7(f)]. In fact, different from dipole gap soliton rotation, the quadruple-like soliton rotation and appearance of DCV states with periodically charge-flipping arise from the superposition of eigenmodes belonging to different high-symmetry points (with different propagation constants) of the third band, as shown theoretically in our earlier work [19].

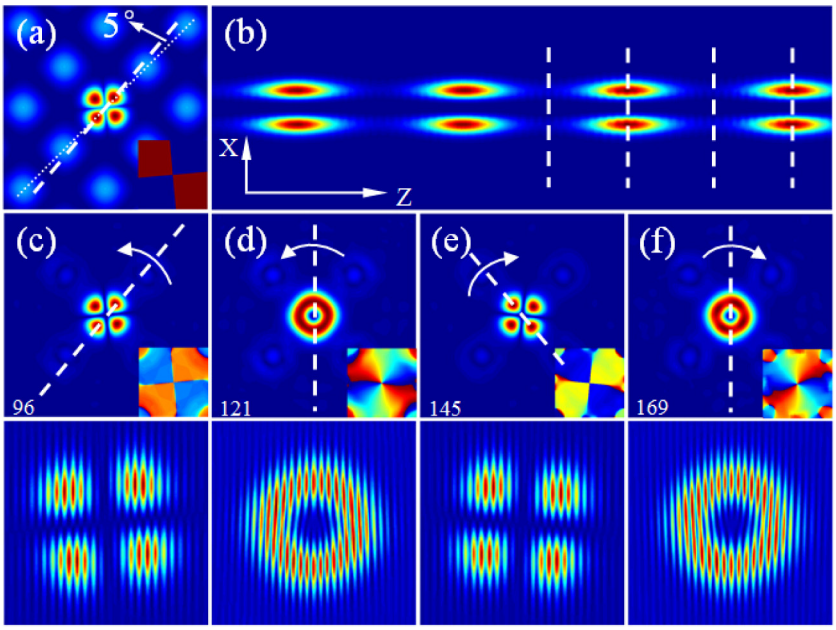

Fig. 7. Numerical results showing self-rotation of higher-band quadruple-like lattice soliton (Media 2). Top row: (a) input quadruple beam superimposed with the lattice pattern. (b) side-view of beam propagation to z = 180mm. Middle row: (c)-(f) nonlinear output intensities corresponding to the locations of white dashed lines in (b). From (c) to (f), z = 96mm, 121mm, 145mm, 169mm. Bottom row: corresponding interferograms of the outputs. In all figures, the inset shows the phase structure where the blue color corresponds to zero phase, the red color corresponds to π phase.

4. Summary

In summary, we have demonstrated self-trapping and rotation of second-band dipole gap solitons as well as third-band quadruple-like gap solitons in 2D square photonic lattices with an appropriate self-focusing nonlinearity. In particular, we have shown that the quadruple-like

#232806 - $15.00 USD Received 21 Jan 2015; revised 7 Feb 2015; accepted 9 Feb 2015; published 11 Feb 2015
© 2015 OSA

soliton residing in the second Bragg reflection gap experiences self-rotation during nonlinear propagation accompanied by transitions between quadruple and DCV states. Our experimental results are corroborated by numerical simulations. This work might prove relevant for the study of higher-band gap soliton dynamics in other discrete nonlinear systems beyond optics.

Acknowledgments

This work was supported by the National Key Basic Research Program of China (2013CB632703, 2013CB328702), the National Natural Science Foundation of China (NSFC) (11304165), International S\&T cooperation program of China (2011DFA52870), International cooperation program of Tianjin (11ZGHHZ01000), and the 111 Project (B07013). ZC acknowledges the support from NSF and AFOSR.

#232806 - $15.00 USD Received 21 Jan 2015; revised 7 Feb 2015; accepted 9 Feb 2015; published 11 Feb 2015
© 2015 OSA